



Reza Yazdanparast · Roham Rafiee 

# A 3D nonlinear viscoelastic–viscoplastic constitutive model for dynamic response of an epoxy resin

Received: 6 May 2024 / Revised: 7 July 2024 / Accepted: 11 August 2024  
© The Author(s), under exclusive licence to Springer-Verlag GmbH Austria, part of Springer Nature 2024

**Abstract** A three-dimensional viscoelastic-viscoplastic constitutive model is presented for predicting the dynamic mechanical behavior of an epoxy resin at low-to-medium strain rates. The model utilizes the generalized Maxwell model, incorporating two Maxwell elements in parallel with a nonlinear spring to represent the viscoelastic response at low and medium strain rates. By utilizing an empirical logarithmic relationship to predict the material properties at different strain rates, a nonlinear exponential relation based on overstress concepts is proposed for modeling the viscoplastic behavior. Comparing the tensile and shear stress–strain curves predicted by the proposed model with the experimentally measured curves, a good agreement is observed. Implementing the viscoelastic-viscoplastic model in commercial finite element software, a three-dimensional numerical discretization is performed. Through simulations of stress-relaxation and loading–unloading tests at various strain rates using the proposed material model, relaxation and hysteresis responses are analyzed. The model successfully predicts the experimentally measured hysteresis response of a specific epoxy resin during the loading cycle, consistent with other nonlinear viscoelastic models. This material model not only well replicates the nonlinear viscoelastic responses below the yield strain but also captures plastic nonlinearities at different strain rates.

## 1 Introduction

Nowadays, due to the increasing emergence of novel materials [1–4] and the effects of various factors such as strain rate and temperature on the behavior of different materials [5–9], there is a growing need to develop new efficient material models. Despite the old history of polymer materials emergence, extensive research is still being conducted due to the high sensitivity of these materials to the loading rates. Depending on the loading rate and its amplitude, these materials may exhibit both viscoelastic and viscoplastic behaviors. Based on numerous experimental observations, the viscoelastic behavior of epoxy resin, which is extensively used in various applications such as aerospace, marine, and automotive industries, is significant even at low strain rates in the elastic strain range up to about 7% [8–11]. For stress ranges exceeding the yield point, viscoplastic behavior emerges with permanent deformation [8–12]. Upon reviewing the literature, three main types of material models have been proposed for these materials: linear/nonlinear viscoelastic, elasto-viscoplastic, and viscoelastic-viscoplastic. Due to the high sensitivity of polymers to the strain rate, even close to the quasi-static range, the modeling of the viscoelastic response of these materials initially received much attention [10]. In this regard, some linear/nonlinear formulations were developed based on the Maxwell model for stress relaxation under constant strain and the Voigt or Kelvin model for creep under constant stress [13, 14]. Since the Maxwell and Kelvin elements alone were not sufficient to describe the behavior of polymeric materials due to the considerable variety of molecular chains, the generalized Maxwell and Kelvin models were further

R. Yazdanparast · R. Rafiee (✉)  
Composites Research Laboratory, Faculty of New Science and Technologies, University of Tehran, Tehran 1439955171, Iran  
e-mail: Roham.Rafiee@ut.ac.ir

established [13, 14]. Thus, the rheological modeling of polymeric materials was described using Maxwell elements in parallel with a spring (also known as the Zener model [13]) or special Kelvin elements in series with a spring or damper [13, 14].

For larger elastic strains where the infinitesimal strain tensor can no longer be used, models based on finite strains were proposed to analyze the nonlinear viscoelastic behavior of these materials [8, 14–17]. Further efforts were made to expand the research frontier of viscoelastic behavior of polymeric materials to higher strain rates [9, 10]. Various experimental studies were conducted on engineering polymeric materials, utilizing the ZWT (Zhu-Wang-Tang) nonlinear viscoelastic constitutive relation for low-to-high-velocity impact loading [9, 10]. By combining two Maxwell elements in parallel with a nonlinear spring, the viscoelastic response of the epoxy resin was modeled for both low and high strain rates [9, 10].

For strains greater than the yield point, the material exhibits distinct characteristics [18]. After yielding, polymeric materials possess a response of strain softening with time-dependent behavior similar to viscosity in a fluid [18, 19]. According to experimental observations [20–22] and the empirical Eyring's model [23], the yield strength increases in a logarithmic manner with increasing strain rate. Hence, inheriting from previous macroscopic [24, 25] and microscopic [26, 27] viscoplastic models established for metals, various models were also developed to describe the behavior of polymeric materials. Shokrieh et al. [28] and Chen and Zhou [11], based on the Johnson–Cook material model [24], and also Goldberg et al. [29, 30] and Shafei and Kiasat [31], based on the Bonder–Partom material model [25], adapted the previous macroscopic viscoplastic models for epoxy resin. Due to microstructural differences, the microscopic models presented for metals are not well developed for polymeric materials [32]. A few models are also presented based on the assumption of a polycrystalline structure for polymer materials [32].

In addition to the two modeling approaches mentioned, more comprehensive models have been developed to describe the viscoelastic and viscoplastic behaviors of polymer materials. Dufour et al. [33] proposed a fully coupled finite strain-based viscoelastic-viscoplastic damage model for epoxy adhesive based on the generalized Maxwell and von Mises plasticity models. Zhu et al. [7] presented a thermodynamically consistent rate-type viscoelastic-viscoplastic constitutive model within the framework of isothermal and small deformation for polymers. According to their one-dimensional rheological model, the viscoelasticity was described by introducing pseudo potentials, and the viscoplastic flows were derived from the directionality hypotheses [7]. Gudimetla and Dori [34] proposed a finite strain viscoelastic-viscoplastic model for polymeric materials based on isotropic and isothermal conditions assumptions. Chen and Smith [12] developed a 3D nonlinear model that was a combination of a nonlinear viscoelastic model and a viscoplastic model based on the von Mises yield criterion and nonlinear kinetic hardening. Zhang et al. [35] proposed a viscoelastic-viscoplastic model using the Drucker–Prager yield function, isotropic and kinematic nonlinear hardening laws, and Perzyna viscosity function for modeling viscoplasticity and a closed-form nonlinear relation to model viscoelasticity. Based on the assumptions of isotropic and small deformation, Liang et al. [5] recently presented a 3D viscoelastic-viscoplastic hybrid model for polymers with an amorphous structure.

It can be seen from the literature survey that various material models have been presented by researchers. However, more comprehensive models are still needed to describe the dynamic behavior of epoxy resin under impact loading. A significant part of the previous models has only addressed the viscoelastic or viscoplastic behavior of epoxy resins within a limited range of strain rates. Recently developed 3D viscoelastic-viscoplastic models are limited to small deformations or low strain rates. However, the current study introduces a nonlinear 3D viscoelastic-viscoplastic model to characterize the behavior of Epon-828 epoxy resin for the ranges of low and medium strain rates. By conducting experimental tests at various strain rates, the tension and shear stress–strain curves of Epon-828 epoxy resin are analyzed to determine the material model parameters. The 3D numerical discretization of the proposed rate-dependent material model is then performed to develop a UMAT subroutine for implementing the proposed material model in ABAQUS software.

## 2 Experiments

This section deals with the experimental determination of tensile and shear properties and behaviors of Epon-828 epoxy resin in the range of low and medium strain rates.

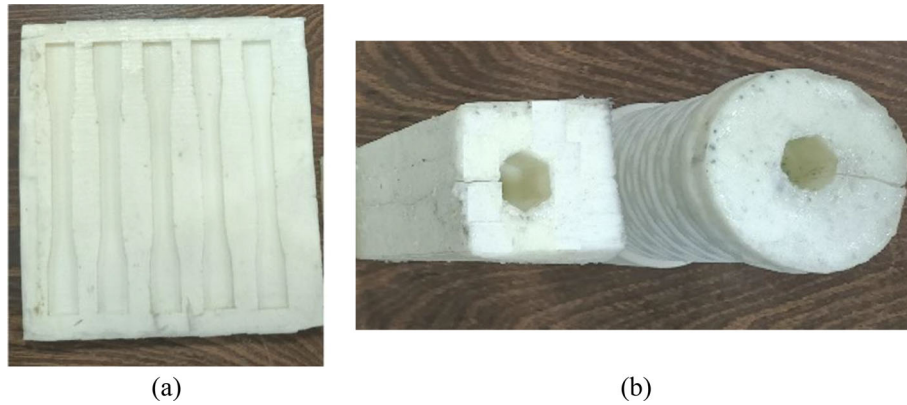


**Fig. 1** Silicone molds for fabricating **a** tensile and **b** shear samples

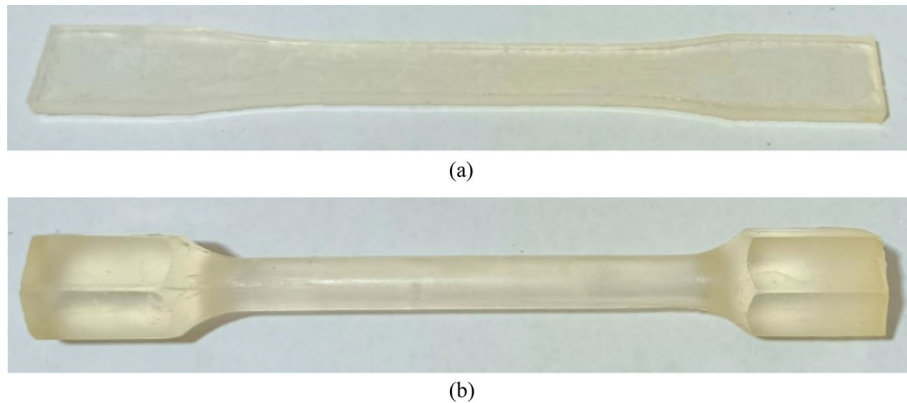


**Fig. 2** **a** Tensile and **b** shear samples made of Epon-828 epoxy resin

### 3 Materials and specimens preparation

The Epon-828 epoxy resin (Di-Glycidyl Ether of Bisphenol A (DGEBA)) with Triethylenetetramine (TETA) hardener at a ratio of 10:1 is used to fabricate the specimens. Silicon molds are utilized for fabricating the specimens as shown in Fig. 1. The specimens are first vacuumed to a pressure of 20 mbar for 30 min for degassing. Then, the samples are cured for two days at room temperature and atmospheric pressure, and subsequently placed in an 80°C oven for 2 h. Figure 2 shows the fabricated testing samples prepared for shear and tensile tests.

### 4 Test procedure

Using a 15-ton-force universal servo-electric tensile machine (see Fig. 3a) in displacement-control mode, the tensile stress–strain curves of epoxy resin were obtained based on ASTM D638-10 [36] for plastic materials. By selecting 15 test samples and allocating 5 of them to perform 5 tensile tests at each tensile speed, experimental measurements were taken at three tensile speeds with strain rates of  $0.0015 \text{ s}^{-1}$ ,  $0.003 \text{ s}^{-1}$ , and  $0.015 \text{ s}^{-1}$ .

For extracting the shear stress–strain curve of epoxy resin, similar to previous studies [28, 29, 37], a torsion testing machine (TecQuipment-SM21, UK) is utilized at three different torsion speeds (see Fig. 3b). By choosing a total of 15 test samples and assigning 5 of them for conducting 5 tests at each torsional speed, measurements were carried out with strain rates of  $0.00015 \text{ s}^{-1}$ ,  $1.5 \text{ s}^{-1}$ , and  $150 \text{ s}^{-1}$ .

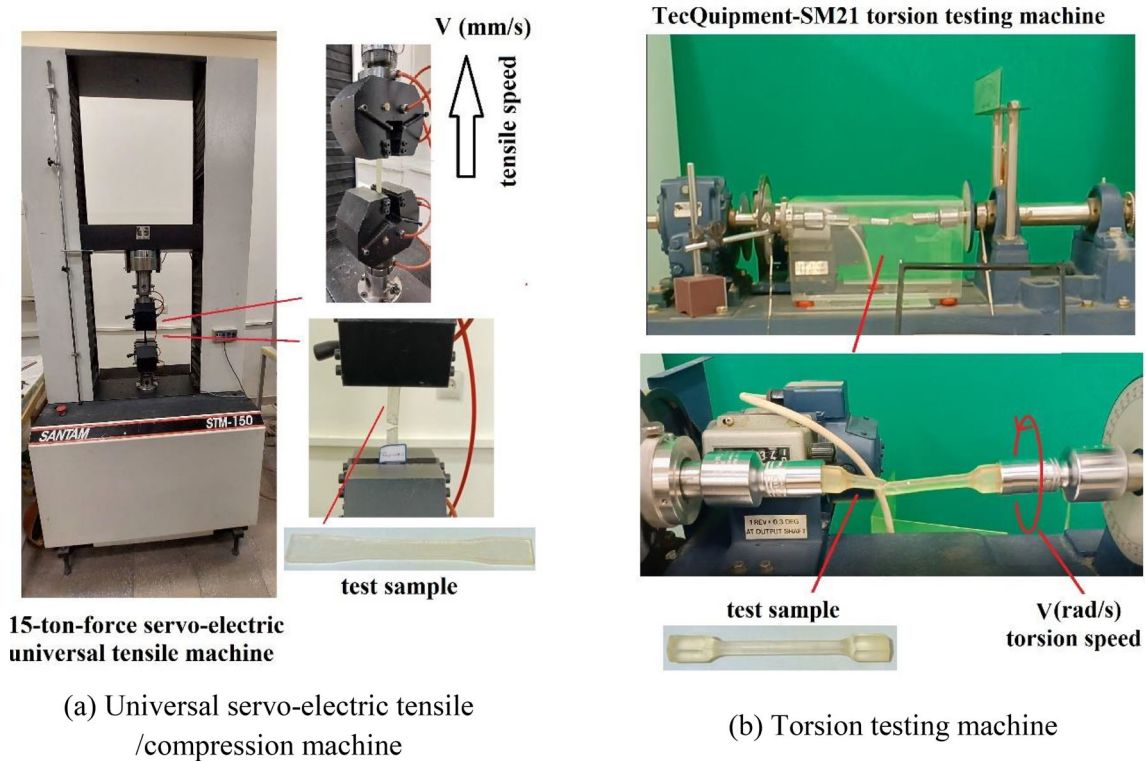


**Fig. 3** Experimental facilities

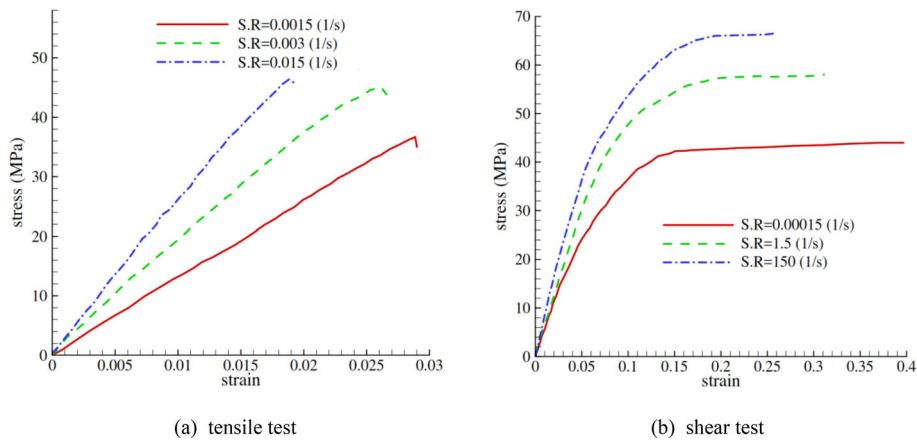


**Fig. 4** Average stress–strain curves for Epon-828 epoxy resin

## 5 Experimental results

The measured average tensile and shear stress–strain curves associated with three different strain rates are shown in Fig. 4. The average stress–strain curve representing the mean of 5 data points at a specific strain is used. Using the obtained curves, the average material properties including tensile/shear modulus ( $E$  and  $G$ ), tensile/shear strength ( $S$ ), and corresponding strain ( $\varepsilon_y$ ) at each strain rate are determined and presented in Table 1.

Referring to Fig. 4, it is evident that as the strain rate increases, the flow stress changes significantly due to an increase in the maximum strength and elastic modulus. Resembling the consistency of presented results with published data in open literature, the dynamic stress–strain curve shifts upwards as the strain rate increases [10, 11, 20, 21, 23, 28, 29, 37–39], leading to a clear difference between dynamic and static stress, known as

**Table 1** Average tensile/shear elastic moduli, maximum stress (strength), and strain at maximum stress

Loading case	Strain rate (1/s)	Modulus (GPa)	Strength (MPa)	Strain at maximum stress
Tensile	0.0015	1.217 ± 0.12	36.07 ± 1.16	0.0287 ± 0.0011
	0.0030	1.938 ± 0.07	45.80 ± 0.95	0.0267 ± 0.0017
	0.015	2.720 ± 0.17	47.71 ± 1.11	0.0189 ± 0.0023
Shear	0.00015	0.553 ± 0.008	43.98 ± 2.43	0.396 ± 0.018
	1.5	0.834 ± 0.013	57.57 ± 1.15	0.308 ± 0.025
	150	0.955 ± 0.013	63.35 ± 3.62	0.263 ± 0.031

**Table 2** Material constants of proposed strain rate-dependent material model

Loading case	Tensile			Shear		
	$f(\varepsilon^o)$	$\varepsilon_y(\varepsilon^o)$	$S(\varepsilon^o)$	$E(\varepsilon^o)$	$\varepsilon_y(\varepsilon^o)$	$S(\varepsilon^o)$
$\alpha$	− 0.00436	− 4.908 × 10 <sup>−11</sup>	5.212 × 10 <sup>−8</sup>	− 0.009617	1.705	0.03537
$\beta$	1	15	9	1	1	1
$\gamma$	0.00077	47.96	2.308	0.3115	55.58	0.7935

overstress or extra stress [10, 20]. Purposefully, in this paper in order to predict the properties of epoxy resin at any desired strain rate, following empirical logarithmic relationship is used:

$$f(\varepsilon^o) = \alpha (\ln(\varepsilon^o))^\beta + \gamma \quad (1)$$

where  $\varepsilon^o$  is strain rate,  $f$  is a desired material property and  $\alpha$ ,  $\beta$  and  $\gamma$  are the material constants. For any desired material property  $f$ , the corresponding material constants can be determined by fitting the logarithmic function of Eq. (1) with the material property values determined experimentally at three different strain rates using Fig. 4 (presented in Table 1). The resulting material constants corresponding to the properties including tensile/shear modulus (E/G), tensile/shear strength (S), and strain at maximum stress ( $\varepsilon_y$ ) are listed in Table 2 for Epon-828 epoxy resin. In this empirical relationship, similar to variations of the well-known Eyring model [23] and the model suggested by Shokrieh et al. [28], peak stress (i.e., strength) is directly proportional to the logarithm of strain rate. Furthermore, the elastic modulus also varies logarithmically with strain rates.

The resulting curves extracted from Eq. (1) for predicting the material properties of Epon-828 epoxy resin in the range of low and medium rates shown in Fig. 5. As it can be seen, the introduced rate-dependent material model (Eq. (1)) is in a good agreement with the experimental measurements and predicts the material properties at any desired strain rate.

## 6 Constitutive model

Acting forces in polymers can arise as a result of intermolecular and molecular network resistances [40]. Energetic intermolecular bond stretching accounts for the elastic (visco) part and thermally activated plastic flow represents the inelastic (visco) part of the total deformation field [40]. Thus, the total strain of polymers can be decomposed into fully recoverable viscoelastic and unrecoverable viscoplastic components assuming that they are decoupled [12, 33, 41].

In this research, a linear viscoelastic model is coupled with a nonlinear viscoplastic model to account for strain rate sensitivity. The behavior of the material is based on the assumption that the rate of deformation is divided into viscoelastic and viscoplastic parts. The viscoelastic model is established based on the generalized Maxwell model, namely two Maxwell elements (including serial spring and damper) in parallel with a spring element are used for modeling viscoelastic response of material at low and medium strain rates. For higher strain ranges where the strain softening is pertinent, a sliding element in the form of two parallel dampers is used to simulate the viscoplastic response resembling the yield surface and overstress concept. Here, the sliding element is fixed until the stress in the material reaches its maximum value (yield stress). When sliding begins, a viscous plastic force develops in the damper element that is proportional to the sliding speed (strain rate).

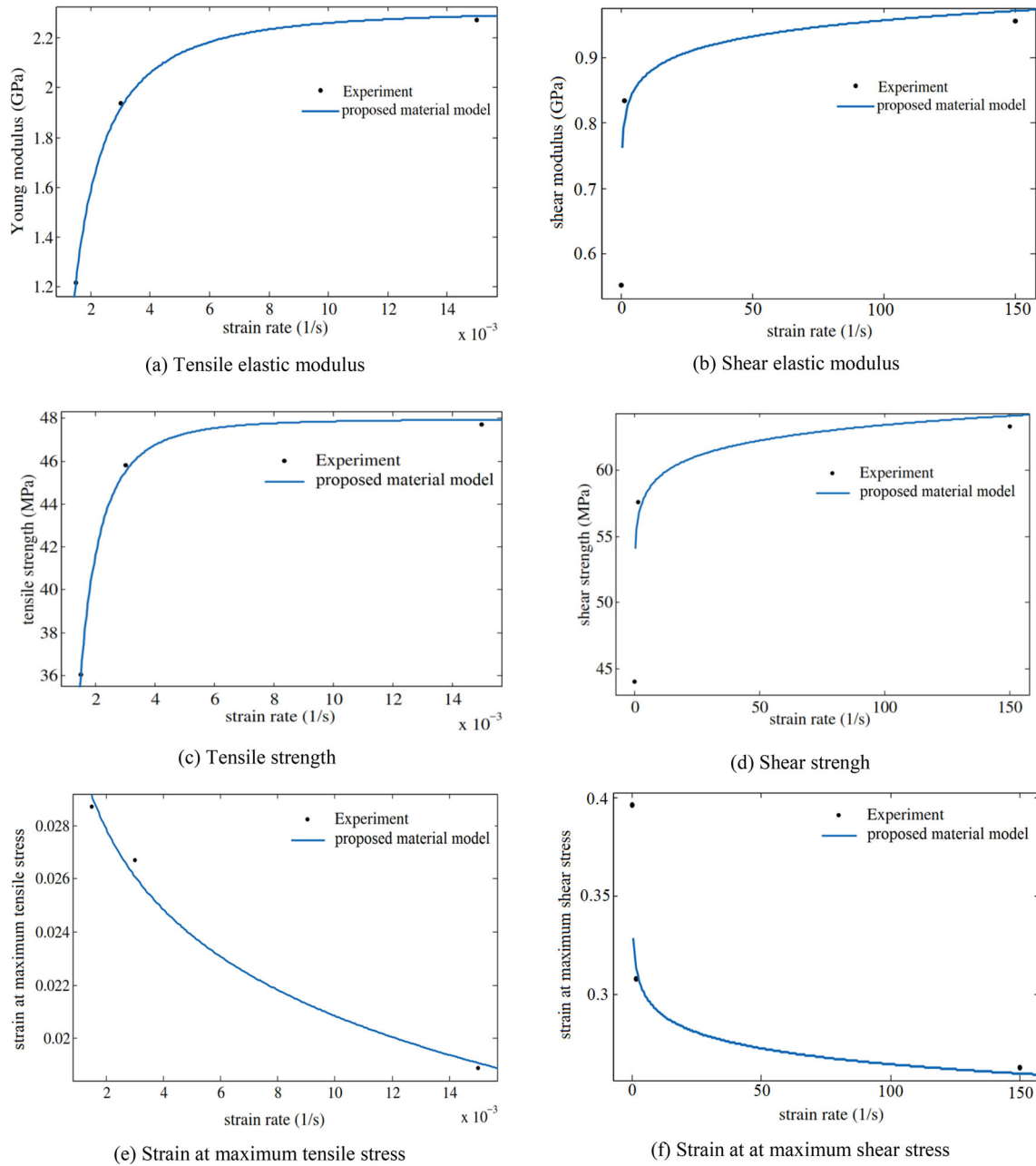


**Fig. 5** Predicted properties at different strain rates in comparison with experimental results

Showing the proposed rheological model in Fig. 6, the resulting constitutive equation for the proposed model is presented as below:

$$\sigma(t) = f(\varepsilon, \varepsilon^o) + \mu_1 \int_0^t \varepsilon^o \exp\left(-\frac{t-\tau}{\tau_1}\right) d\tau + \mu_2 \int_0^t \varepsilon^o \exp\left(-\frac{t-\tau}{\tau_2}\right) d\tau \quad (2)$$

where  $\tau_1$  and  $\tau_2$  are the relaxation times corresponding to the viscoelastic response of the epoxy resin at low and high strain rates, respectively.  $\mu_1$  and  $\mu_2$  refer to the elastic constants of two Maxwell elements. The first

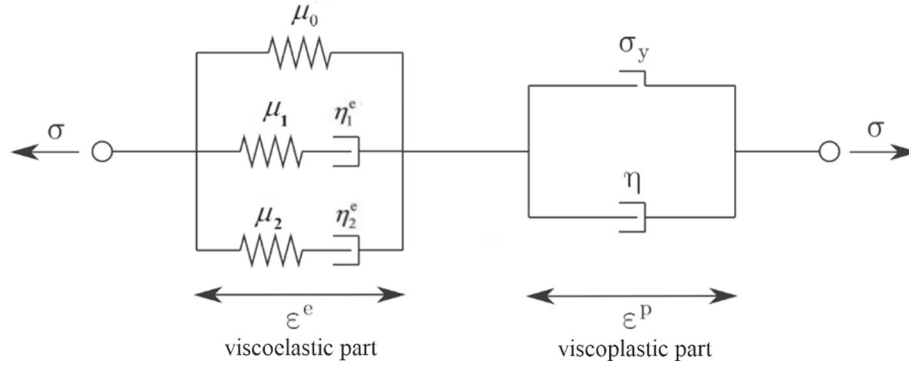


**Fig. 6** Rheological model for viscoelastic-viscoplastic behavior

part of this relationship represents the elasto-viscoplastic response of epoxy resin and is expressed in the form of a nonlinear exponential relation as follows:

$$f(\varepsilon, \varepsilon^o) = \mu_0 \varepsilon^p e^{[-f \times (\varepsilon/\varepsilon_y)^q]} \quad (3)$$

where  $\mu_0$  is the elastic constant of the material and  $p$  is the strain hardening factor. The exponential part of the relation represents the viscoplastic behavior of the material, where  $f$  is the overstress coefficient representing the difference in stress at any desired strain rate relative to the strain rate of  $\varepsilon_0$ , i.e., quasi-static strain.  $\varepsilon_y$  is the strain associated with the maximum stress and  $q$  is a strain factor. Since the material properties of  $\mu_0$  and  $\varepsilon_y$  used in Eq. (3) depend on strain rate according to the logarithmic-based relation (Eq. (1)), the proposed VE-VP material model in this paper exhibited nonlinear behavior at different strain rates.

## 7 Numerical formulation

3D numerical form of Eq. (2) needs to be developed in order to implement it in the commercial Finite Element (FE) package Abaqus as a User Material (UMAT) subroutine. This is done based on the discretization technique by Kaliske and Rothert [42]. For this purpose, Eq. (2) is rewritten as

$$\sigma(t) = \mu_0 \varepsilon^p e^{[-f \times (\varepsilon/\varepsilon_y)^q]} + \int_0^t \sum_{i=1}^2 \mu_i \exp\left(-\frac{t-s}{\tau_i}\right) \frac{\partial \varepsilon(s)}{\partial s} ds \quad (4)$$

which can be shortened to the general form:

$$\sigma(t) = \sigma_0(t) + \sum_{i=1}^2 h_i(t) \quad (5)$$

In this equation,  $\sigma_0(t)$  represents the stress related to the nonlinear elasto-viscoplastic term, and  $h_i(t)$  is the internal stress in two Maxwell elements. Considering linear springs for Maxwell elements where  $\varepsilon(s) = \sigma(s)/\mu_i$ ,  $h_i(t)$  can be rewritten in terms of stress using Eqs. (4) and (5) as follows [42]:

$$h_i(t) = \int_0^t \exp\left(-\frac{t-s}{\tau_i}\right) \frac{\partial \sigma(s)}{\partial s} ds \quad (6)$$

In this formulation,  $h_i(t)$  can be determined as a state variable at different time steps using the finite difference method. Hence, for time 0 to  $t_{n+1}$ , it can be expressed as follows [42]:

$$h_i(t_{n+1}) = \int_0^{t_n} \exp\left(-\frac{t_{n+1}-s}{\tau_i}\right) \frac{d\sigma(s)}{ds} ds + \int_{t_n}^{t_{n+1}} \exp\left(-\frac{t_{n+1}-s}{\tau_i}\right) \frac{d\sigma(s)}{ds} ds \quad (7)$$

For an arbitrary time interval  $[t_n, t_{n+1}]$  with a time step  $\Delta t = t_{n+1} - t_n$ , one can write:

$$\exp\left(-\frac{t_{n+1}}{\tau_i}\right) = \exp\left(-\frac{t_n + \Delta t}{\tau_i}\right) = \exp\left(-\frac{t_n}{\tau_i}\right) \exp\left(-\frac{\Delta t}{\tau_i}\right) \quad (8)$$

Consequently, Eq. (7) can be also simplified to [42]:

$$h_i(t_{n+1}) = \exp\left(-\frac{\Delta t}{\tau_i}\right)h_i(t_n) + \int_{t_n}^{t_{n+1}} \exp\left(-\frac{t_{n+1}-s}{\tau_i}\right) \frac{d\sigma(s)}{ds} ds \quad (9)$$

Meanwhile, it can be expressed using a simple finite difference technique as:

$$\frac{d\sigma(s)}{ds} = \lim_{\Delta s \rightarrow 0} \left( \frac{\Delta\sigma(s)}{\Delta s} \right) = \lim_{\Delta s \rightarrow 0} \left( \frac{\sigma^{n+1} - \sigma^n}{\Delta s} \right) \quad (10)$$

Thus, the time discrete form of Eq. (9) is resulted in following equation [42]:

$$h_i^{n+1} = \exp\left(-\frac{\Delta t}{\tau_i}\right)h_i^n + \frac{1 - \exp\left(-\frac{\Delta t}{\tau_i}\right)}{\frac{\Delta t}{\tau_i}} (\sigma^{n+1} - \sigma^n) \quad (11)$$

Finally, we have:

$$h_i^{n+1} = \exp\left(-\frac{\Delta t}{\tau_i}\right)h_i^n + \frac{1 - \exp\left(-\frac{\Delta t}{\tau_i}\right)}{\frac{\Delta t}{\tau_i}} (C_{MK}^e \varepsilon^{n+1} - C_{MK}^e \varepsilon^n) \quad (12)$$

Therefore, knowing  $h_i(t)$  at the current time step, its value for the next time step can be obtained. Then, the 3D form of Eq. (2) can be expressed as below based on the iterative formula:

$$\sigma_M^{n+1} = \mu_0 \varepsilon^p e^{\left[-f \times \left(\frac{\varepsilon}{\varepsilon_y}\right)^q\right]} + \sum_{j=1}^2 \left( h_j^n e^{\left(-\frac{\Delta t}{\tau_j}\right)} + \tau_j \frac{1 - e^{\left(-\frac{\Delta t}{\tau_j}\right)}}{\Delta t} [C_{MK}^e \varepsilon_K^{n+1} - C_{MK}^e \varepsilon_K^n] \right) \quad (13)$$

Here, using Eq. (13) the Jacobian modulus or material tangent required for developing the UMAT subroutine can be expressed as follows [43]:

$$\mathbb{C}^{n+1} = \frac{\partial \Delta \sigma}{\partial \Delta \varepsilon} = \left\{ 1 + \sum_{j=1}^2 \frac{1 - \exp\left(-\frac{\Delta t}{\tau_j}\right)}{\frac{\Delta t}{\tau_j}} \right\} \mathbb{C}^{n+1} \quad (14)$$

where  $\Delta \sigma$  is a small increment in Cauchy stress,  $\Delta \varepsilon$  is the increment in strain, and  $\mathbb{C}$  is the stiffness matrix defined as following:

$$C_{KM} = D(i, j) = \begin{bmatrix} K + \frac{4}{3}\mu_0 & K - \frac{2}{3}\mu_0 & K - \frac{2}{3}\mu_0 & 0 & 0 & 0 \\ K - \frac{2}{3}\mu_0 & K + \frac{4}{3}\mu_0 & K - \frac{2}{3}\mu_0 & 0 & 0 & 0 \\ K - \frac{2}{3}\mu_0 & K - \frac{2}{3}\mu_0 & K + \frac{4}{3}\mu_0 & 0 & 0 & 0 \\ 0 & 0 & 0 & \mu_0 & 0 & 0 \\ 0 & 0 & 0 & 0 & \mu_0 & 0 \\ 0 & 0 & 0 & 0 & 0 & \mu_0 \end{bmatrix} \quad (15)$$

when  $K$  represents the bulk modulus of the epoxy resin.



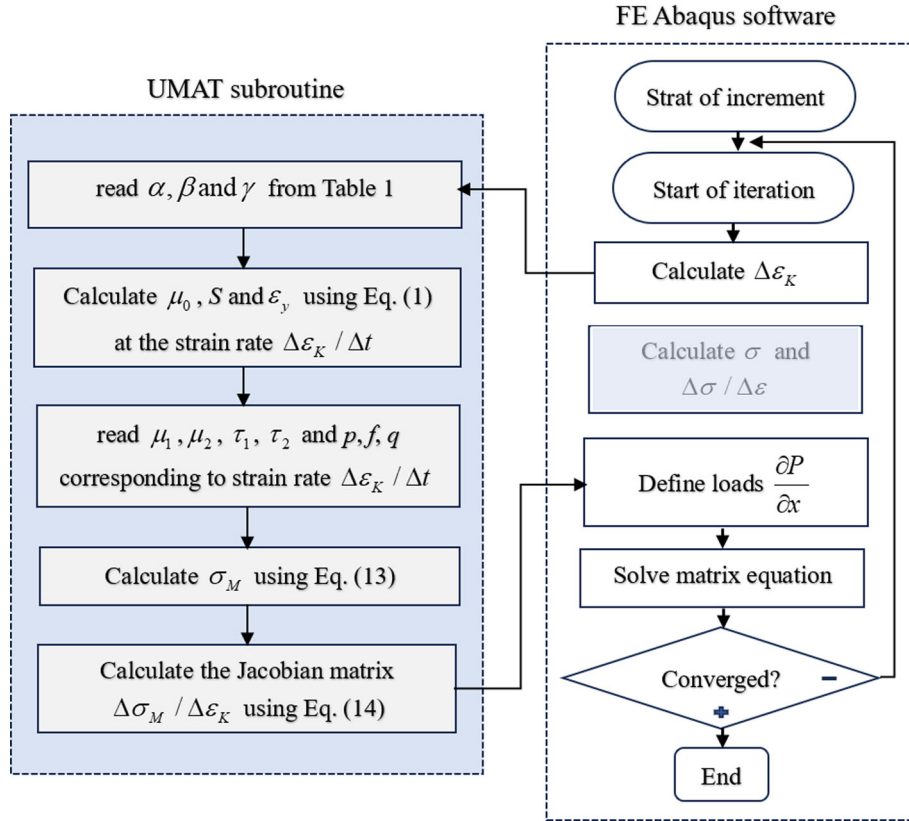


Fig. 7 Flow chart of the UMAT subroutine interacting with the FE Abaqus/Standard

## 8 Implementing in the FE software

This section provides details on the implementation of the 3D rate-dependent proposed material model through the UAMT subroutine interacting with the FE Abaqus/Standard software, as shown in Fig. 7. This subroutine returns the updated stress tensor and Jacobian matrix to the Abaqus/Standard software for any small increment of strain  $\Delta\epsilon_K$ , at a time increment  $\Delta t$ , using Eqs. (13) and (14) respectively, through the following steps:

1. Reads the known material constants  $\alpha$ ,  $\beta$  and  $\gamma$  from Table 1.
2. Calculates the elastic modulus (E/G), strength (S), and strain at maximum stress  $\epsilon_y$  using Eq. (1) at the given strain rate  $\Delta\epsilon_K / \Delta t$ ,
3. Reads the known material model parameters  $\mu_1, \mu_2, \tau_1, \tau_2, q, p$ , and  $f$  at the given strain rate  $\Delta\epsilon_K / \Delta t$ .
4. Calculates the new updated stress tensor  $\sigma_M$  using Eq. (13),
5. Calculates the Jacobian matrix  $\Delta\sigma / \Delta\epsilon$  using Eq. (14).

## 9 Results and discussion

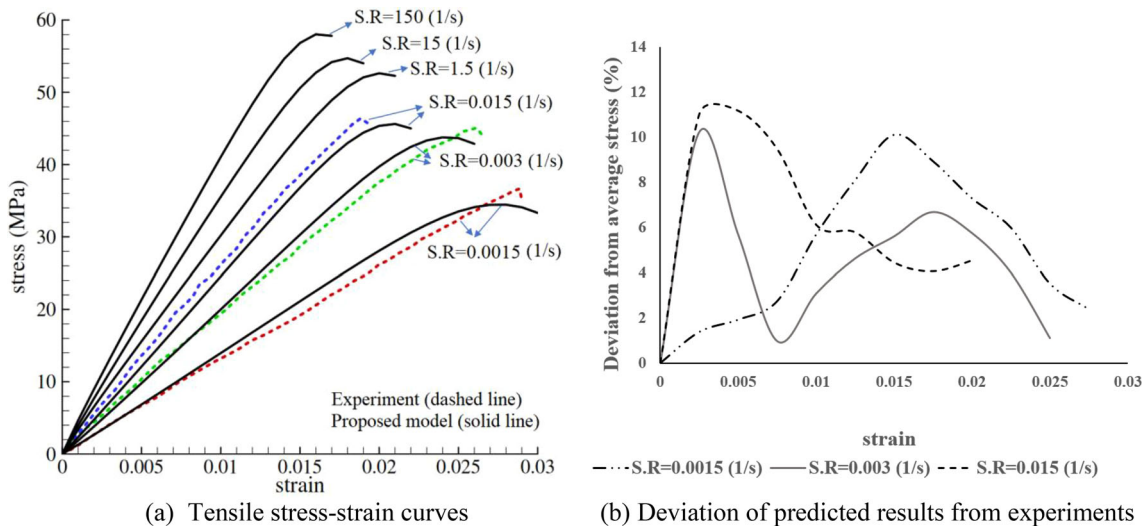
In this section, the proposed viscoelastic-viscoplastic constitutive model is first evaluated by comparing the predicted dynamic mechanical behavior of epoxy resin with experimental data. Subsequently, the accuracy of the implemented 3D numerical formulation for the proposed material model and the resulting UMAT subroutine is examined.

## 10 Validation of proposed material model

The parameters of the model described by Eq. (2) are obtained through the curve-fitting process of proposed constitutive models to experimental results. The material constants of relaxation times associated with low and

**Table 3** Material constants of proposed viscoelastic-viscoplastic model

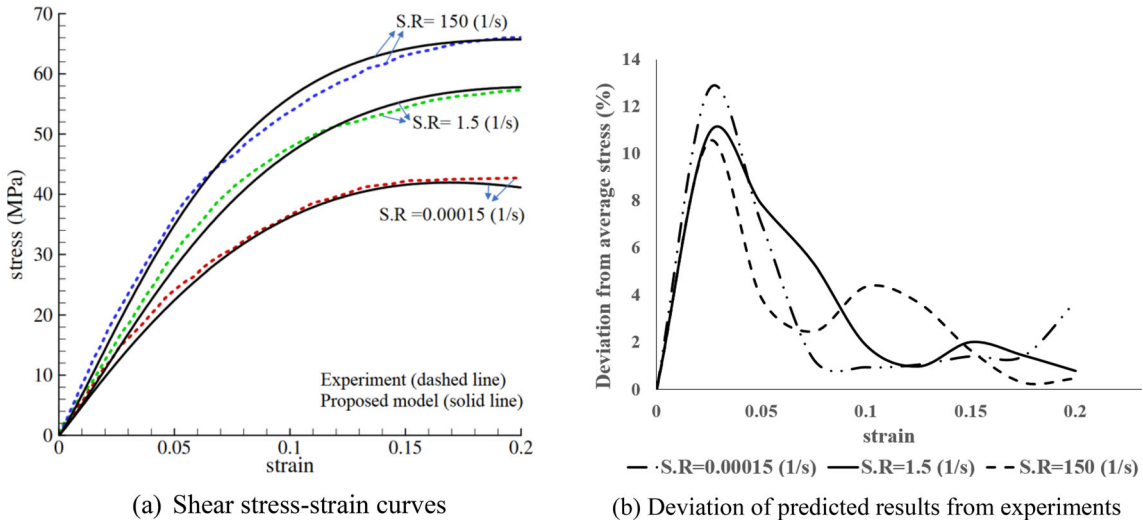
Loading type	f	p	q	$\varepsilon_0^o$	E1 (GPa)	E2 (GPa)	$\tau_1$ (s)	$\tau_2$ (s)
Tensile	$\frac{\varepsilon^o}{\varepsilon_0^o} (0.85 + 0.05 \ln(\frac{\varepsilon^o}{\varepsilon_0^o})) + 0.6 \left  \log_{10}(\frac{\varepsilon^o}{\varepsilon_0^o}) \right  (\frac{\varepsilon^o}{10^5 \varepsilon_0^o})^{0.3}$	$1.05 - 0.01 \ln(\varepsilon^o/\varepsilon_0^o)$	8	0.0015	0.437	0.437	0.0001	108
Shear	2.6642	$1.25 - 0.1 \varepsilon^o/\varepsilon_0^o$	1.2	0.00015	0.120	0.120	0.0001	108

**Fig. 8** Prediction of tensile stress–strain curves by the proposed model in comparison with experimental measurements

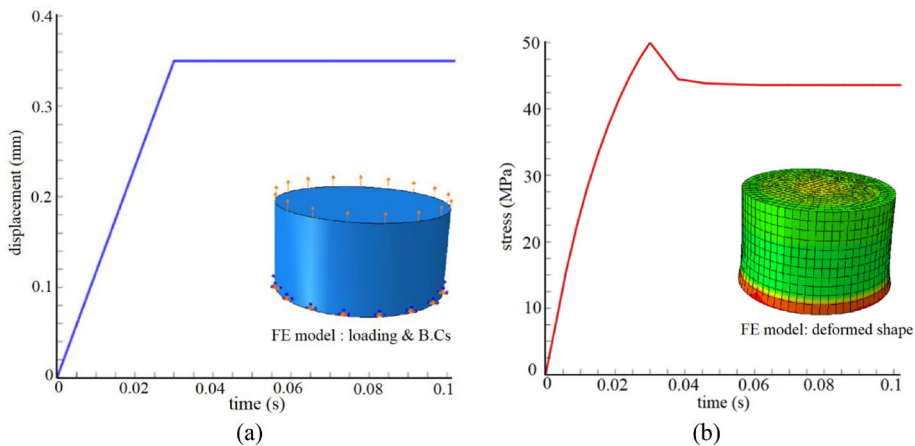
high strain rates are set at  $\tau_1 = 108$  s and  $\tau_2 = 0.0001$  s, respectively, based on experiments conducted by Wang et al. [10] on epoxy resin. Extensive dynamic tests on epoxy resin concluded that the relaxation time for low strain rates falls within the range of  $10^{-6}$ – $10^2$  s, while for high strain rates (impact loading), it falls within the range of  $10^{-6}$ – $10^{-4}$  s [10]. The parameters obtained for the proposed model are listed in Table 3.

Figure 8a shows the predicted stress–strain curve using the proposed constitutive material model for various strain rates, ranging from low to medium. The accuracy of the material model is evaluated by comparing the predicted results with the average stress–strain curves extracted experimentally at three strain rates of  $0.0015$  s $^{-1}$ ,  $0.003$  s $^{-1}$ , and  $0.015$  s $^{-1}$ . It can be seen that the proposed model (solid line) predicts the behavior of epoxy resin very well from elastic to plastic deformation until strain softening occurs which is consistent with the average stress–strain curve (dashed line) presented in Fig. 4a. For three strain rates of  $0.0015$  s $^{-1}$ ,  $0.003$  s $^{-1}$ , and  $0.015$  s $^{-1}$ , the deviation of the estimated strain–stress curve by the proposed model from the average stress–strain curve of epoxy resin is shown in Fig. 8b. Comparing the predicted stress with the corresponding experimentally measured data (average stress) at the same strain ranges, a maximum deviation of about 11.5% can be observed across all strain ranges. By ensuring the accuracy of the proposed constitutive model in estimating material behavior for low strain rates, this model further predicted the stress–strain curves in the medium strain rate range (from  $0.015$  s $^{-1}$  up to  $150$  s $^{-1}$ ) as shown in Fig. 8a.

Similarly, as shown in Fig. 9a, under shear loading, the proposed model (solid line) approximates the elastic and plastic behavior of epoxy resin in accordance with the average stress–strain curve (dashed line) measured experimentally (as shown in Fig. 4b). According to Fig. 9b, for three strain rates of  $0.00015$  s $^{-1}$ ,  $1.5$  s $^{-1}$ , and  $150$  s $^{-1}$ , the deviation of the estimated strain–stress curve by the proposed model from the averaged stress–strain curve is lower by approximately 12% across all strain ranges. Although the observed discrepancy between the predicted and experimental curves may be noticeable at very low strains, it decreases to less than 4% as the strain increases. Achieving the appropriate agreement between the shear stress–strain curves predicted by the proposed constitutive model and the experimental measurements, the presented material model facilitates



**Fig. 9** Prediction of shear stress–strain curves by the proposed model compared to experimental measurements



**Fig. 10** **a** Loading profile applied to the FE model and **b** the resulting stress-relaxation response

the estimation of the shear behavior of epoxy resin for any arbitrary strain rate up to  $150 \text{ s}^{-1}$  with reliable accuracy.

### 11 Verification of numerical modeling

In order to ensure the proper performance of the developed 3D numerical formulation, the viscous behavior of Epon-828 epoxy resin is evaluated in this section. For this purpose, the stress-relaxation test and hysteresis behavior of the investigated resin are simulated based on the proposed material model using the developed UMAT subroutine in the commercial FE package of Abaqus.

Simulating the stress-relaxation test involves applying a strain at a constant rate along the axis of a cylinder with a diameter of 12.7 mm and a length of 3 mm for a short time of  $t_0 = 0.03 \text{ s}$  until it reaches a maximum value. Subsequently, the strain is maintained constant, as illustrated in Fig. 10a. The FE model of this cylinder, fixed at one end and deforming at the other end, is shown in Fig. 10a. The resulting deformed shape of this FE model is depicted in Fig. 10b. Referring to Fig. 10b, as the strain increases, the stress initially reaches its maximum value at time  $t_0$ . After the strain reaches to a constant value, the stress starts decreasing exponentially with a noticeable lag until it also becomes constant at  $t_0 = 0.1 \text{ s}$ . As it can be seen, the 3D material model used in the simulation demonstrates a rational response, since it properly captures the stress-relaxation behavior.

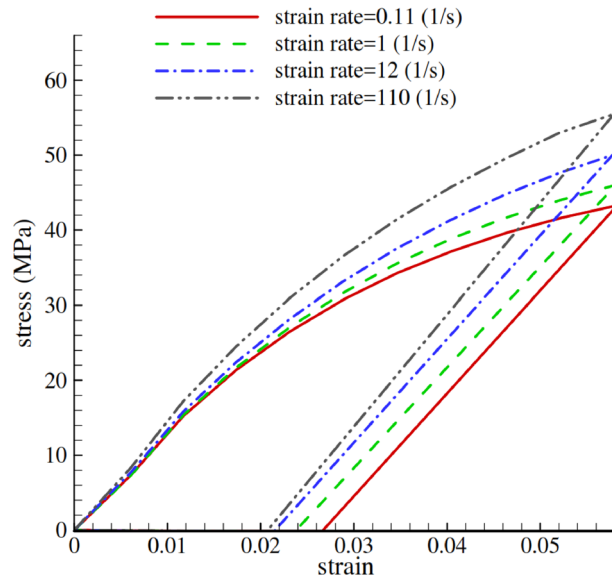


**Fig. 11** Predicted hysteresis curve of Epon-828 epoxy resin at different strain rates

For materials with nonlinear viscoelastic behavior, in loading and unloading conditions, the stress and strain curves are different and form the hysteresis curve [10, 44]. For more accurate description of the polymeric materials behavior with dominant nonlinear viscoelastic behavior, it is suitable to examine the constitutive equation in two states of loading and unloading conditions. The 3D numerical implementation of the proposed model is investigated to show the hysteresis behavior caused by the viscoelastic properties of Epon-828 resin. For this purpose, a strain with constant rates is applied along the longitudinal axis of the cylindrical sample used in the stress-relaxation test, and then it is suddenly unloaded. Figure 11 shows the resulting stress–strain curves at different strain rates for both loading and unloading conditions. It can be seen that the hysteresis behavior of the epoxy resin is well predicted by the 3D material model developed in the UMAT subroutine.

To verify the accuracy and universality of the proposed 3D numerical material model for a particular epoxy resin, the hysteresis behavior is predicted and compared with the response of various VE material models and experimental data. Xia et al. [45] conducted cyclic uniaxial loading/unloading tests to extract the hysteresis behavior of an epoxy polymer (Epon 826/Epi-Cure 9551) in order to evaluate the predictive capabilities of three basic types of nonlinear viscoelastic constitutive models. They chose a mechanical analog model in differential form [46], a modified Schapery's model based on nonequilibrium thermodynamics in integral form [47], and a modified Knauss-Emri free volume model, also in integral form [48]. Considering  $\tau_1 = 1$  s,  $\tau_2 = 10$  s,  $\mu_1 = 12.8293$  MPa,  $\mu_2 = 44.5651$  MPa, and  $\mu_0 = 2129$  MPa for this type of epoxy resin [45], the resulting hysteresis response predicted by the proposed 3D numerical method and three previous nonlinear viscoelastic models [46–48] are shown in Fig. 12 accompanied with the experimental data [45] at a strain rate of  $1.5 \times 10^{-5} \text{ s}^{-1}$ . The hysteresis simulation is conducted on a solid cylindrical specimen with the same geometry and loading conditions as those used in the uniaxial loading/unloading test by a servo-controlled electrohydraulic test machine [45, 46, 49]. It can be observed that, similar to the other three nonlinear VE models and experimental data, the slope (tangent modulus) of the loading branch decreases with increasing stress. However, the trend is reversed in the unloading phase. Referring to this figure again, it is evident that through all loading/unloading cycles, the proposed 3D viscoelastic model, similar to the modified free volume model [48], remarkably predicts the experimental data during both loading and unloading phases better than the modified analog [46] and thermodynamic [47] models. Due to establishing the VE response of the proposed material model and the modified free volume model based on the generalized Maxwell method, the hysteresis response obtained is nearly identical.

In comparison with the previous nonlinear VE models, the proposed material model not only estimates the VE response of a material under yield strain but also considers the VP response of epoxy resin in the plastic region at low-to-medium strain rates. This model is suitable for low-to-medium strain rates, unlike many previous viscoelastic, elasto-viscoplastic, and recently developed 3D viscoelastic-viscoplastic models for epoxy resins, which were developed only for a range of low strain rates. This developed 3D VE-VP material

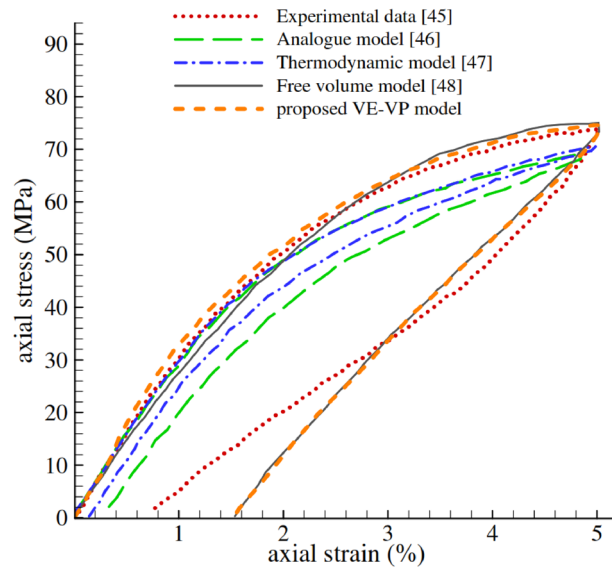


**Fig. 12** The predicted hysteresis curve by the proposed material model and other theoretical models [46–48], in comparison to experimental data [45]

model; however, is accompanied by some limitations and assumptions. It assumes the same axial properties for epoxy resin in both tensile and compressive directions. It is developed at standard room temperature, making it suitable for situations where the effect of temperature on the material behavior of epoxy resin is not significant. For applying this model at higher strain rates and different temperatures, new experimental data are needed to characterize the proposed material model.

## 12 Conclusion

The dynamic mechanical behavior of an epoxy resin as a matrix phase is studied experimentally and numerically. An empirical constitutive model is proposed to predict material properties at different strain rates for an epoxy resin, taking into account its viscoelastic-viscoplastic behavior. According to the presented results, for epoxy resin at standard room temperature, the dynamic stress–strain curve can be divided into three stages: initial elastic, yield, and strain softening. The elastic modulus and strength of Epon-828 epoxy resin increase logarithmically with increasing strain rate, while the strain at maximum stress decreases logarithmically. By comparing the predicted tensile and shear stress–strain curves with the experimentally measured ones at the corresponding strain rates, a good agreement between the results is observed in the entire range of elastic and plastic deformation. FE simulations of stress-relaxation and loading–unloading tests, based on the proposed material model, demonstrate a reasonable prediction of the expected relaxation and hysteresis behavior of epoxy resin. Therefore, it can be concluded that the proposed material model and its 3D discretized form provide a reasonable estimate of the dynamic material behavior for Epon-828 epoxy resin within the range of low-to-medium strain rates.

**Acknowledgements** The authors acknowledge the financial support provided by the Iranian National Science Foundation (INSF) under contract 4003498.

**Data availability** The datasets generated and/or analyzed during the current study are available from the corresponding author on reasonable request.

## Declarations

**Conflict of interest** The authors have no relevant financial or non-financial interests to disclose.

## References

- Shi, P., Chen, Y., Feng, J., Sareh, P.: Highly stretchable graphene kirigami with tunable mechanical properties. *Phys. Rev. E* **109**(3), 035002 (2024)
- Chen, Y., He, R., Hu, S., Zeng, Z., Guo, T., Feng, J., Sareh, P.: Design–material transition threshold of ribbon kirigami. *Mater. Des.* **242**, 112979 (2024)
- Jalali, E., Soltanizadeh, H., Chen, Y., Xie, Y.M., Sareh, P.: Selective hinge removal strategy for architecting hierarchical auxetic metamaterials. *Commun. Mater.* **3**(1), 97 (2022)
- Fan, L., Sun, Y., Fan, W., Chen, Y., Feng, J.: Determination of active members and zero-stress states for symmetric prestressed cable–strut structures. *Acta Mech.* **231**, 3607–3620 (2020)
- Liang, Z., Li, J., Zhang, X., Kan, Q.: A viscoelastic-viscoplastic constitutive model and its finite element implementation of amorphous polymers. *Polym. Testing* **117**, 107831 (2023)
- Colaka, O.U., Cakir, Y.: Material model parameter estimation with genetic algorithm optimization method and modeling of strain and temperature dependent behavior of epoxy resin with cooperative-VBO model. *Mech. Mater.* **135**, 57–66 (2019)
- Zhu, Y., Lu, F., Yu, C., Kang, G.: A rate-type nonlinear viscoelastic–viscoplastic cyclic constitutive model for polymers: theory and application. *Polym. Eng. Sci.* **56**(12), 1375–1381 (2016)
- Tamrakar, S., Ganesh, R., Sockalingam, S., Haque, B.Z.G., Gillespie, J.W.: Strain rate-dependent large deformation inelastic behavior of an epoxy resin. *J. Comp. Mater.* **54**(1), 71–87 (2020)
- Luo, G., Wu, C., Xu, K., Liu, L., Chen, W.: Development of dynamic constitutive model of epoxy resin considering temperature and strain rate effects using experimental methods. *Mech. Mater.* **159**, 103887 (2021)
- Wang, L., Yang, L., Dong, X., Jiang, X.: *Dynamics of Materials: Experiments, Models and Applications*, 1st edn. Elsevier Academic Press, Cambridge (2019)
- Chen, W., Zhou, B.: Constitutive behavior of epon 828/T-403 at various strain rates. *Mech. Time-Depend. Mater.* **2**, 103–111 (1998)
- Chen, Y., Smith, L.V.: A nonlinear viscoelastic–viscoplastic constitutive model for adhesives under creep. *Mech. Time-Depend. Mater.* **26**(3), 663–681 (2022)
- Liu, X., Li, D.: A link between a variable-order fractional Zener model and non-Newtonian time-varying viscosity for viscoelastic material: relaxation time. *Acta Mech.* **232**, 1–13 (2021)
- Shabana, A.A.: *Computational Continuum Mechanics*, 2ed edn., p. 9781107016026. Cambridge University Press, Cambridge (2011)
- Lockett, F.J.: *Nonlinear Viscoelastic Solids*, p. 0124543502. Academic Press, London (1972)
- O’Dowd, N.P., Knauss, W.G.: Time dependent large principal deformation of polymers. *J. Mech. Phys. Solids* **43**(5), 771–792 (1995)
- Hayashi, E.Y., Coda, H.B.: Alternative finite strain viscoelastic models: constant and strain rate-dependent viscosity. *Acta Mech.* **235**, 3699–3719 (2024)
- Boyce, M.C., Parks, D.M., Argon, A.S.: large inelastic deformation of glassy polymers part i: rate dependent constitutive model. *Mech. Mater.* **7**(1), 15–33 (1988)
- Mizuno, M., Sanomura, Y.: Phenomenological formulation of viscoplastic constitutive equation for polyethylene by taking into account strain recovery during unloading. *Acta Mech.* **207**, 83–93 (2009)
- Davies, E.D.H., Hunter, S.C.: The dynamic compression testing of solids by the method of the split Hopkinson pressure bar. *J. Mech. Phys. Solids* **11**(3), 155–179 (1963)
- Chou, S.C., Robertson, K.D., Rainey, J.H.: The effect of strain rate and heat developed during deformation on the stress-strain curve of plastics. *Exp. Mech.* **13**, 422–432 (1973)
- Trojanowski, A., Ruiz, C., Harding, J.: Thermomechanical properties of polymers at high rates of strain. *J. Phys. IV* **7**, 447–452 (1997)
- Ward, I.M., Sweeney, J.: *Mechanical Properties of Solid Polymers*, 3rd edn., p. 9781444319507. John Wiley & Sons Ltd, Hoboken (2012)
- Johnson, G.R., Hoegfeldt, J.M., Lindholm, U.S., Nagy, A.: Response of various metals to large torsional strains over a large range of strain rates e part I: ductile metals. *J. Eng. Mater. Technol.* **105**(1), 42–47 (1983)
- Bodner, S.R., Partom, Y.: Constitutive equations for elastic-viscoplastic strain hardening materials. *J. Appl. Mech.* **42**, 385–389 (1975)
- Seeger, A., CXXXII: The generation of lattice defects by moving dislocations, and its application to the temperature dependence of the flow-stress of FCC crystals. *London, Edinburgh, and Dublin Philosophical Magazine and J. Sci.* **46**(382), 1194–1217 (1955)
- Zerilli, F.J., Armstrong, R.W.: Dislocation-mechanics-based constitutive relations for material dynamics calculations. *J. Appl. Phys.* **61**(5), 1816–1825 (1987)
- Shokrieh, M.M., Shamaei Kashani, A.R., Mosalmani, R.: A dynamic constitutive micromechanical model to predict the strain rate dependent mechanical behavior of carbon nanofiber/ epoxy nanocomposites. *Iran. Polym. J.* **25**(6), 487–501 (2016)
- Goldberg, R.K., Roberts, G.D., Gilat, A.: Implementation of an associative flow rule including hydrostatic stress effects into the high strain rate deformation analysis of polymer matrix composites. *J. Aerosp. Eng.* **18**(1), 18–27 (2005)
- Poulain, X., Benzerga, A.A., Goldberg, R.K.: Finite-strain elasto-viscoplastic behavior of an epoxy resin: experiments and modeling in the glassy regime. *Int. J. Plast.* **62**, 138–161 (2014)
- Shafiei, E., Kiasat, M.S.: A new viscoplastic model and experimental characterization for thermosetting resins. *Polym. Testing* **84**, 106389 (2020)
- Meyer, A., Murr, L.E., Staudhammer, K.P.: *Shock-Wave and High-Strain-Rate Phenomena in Materials*, p. 0824785797. Marcel Dekker Inc., New York (1992)
- Dufour, L., Bourel, B., Lauro, F., Haugou, G., Leconte, N.: A viscoelastic– viscoplastic model with non-associative plasticity for the modelling of bonded joints at high strain rates. *Int. J. Adhes. Adhes.* **70**, 304–314 (2016)

34. Gudimetla, M.R., Doghri, I.: A finite strain thermodynamically-based constitutive framework coupling viscoelasticity and visco-plasticity with application to glassy polymers. *Int. J. Plast.* **98**, 197–216 (2017)
35. Zhang, L., Klimm, W.J., Kwok, K., Yu, W., A nonlinear viscoelastic-viscoplastic constitutive model for epoxy polymers, American Institute of Aeronautics and Astronautics, Conference Paper (2022)
36. ASTM D638-10, Standard Test Method for Tensile Properties of Plastics. (2014)
37. Goldberg, R.K., Roberts, G.D. and Gilat, A.: Strain rate sensitivity of epoxy resin in tensile and shear loading, NASA/TM—2005-213595, (2005)
38. Briscoe, B.J., Nosker, R.W.: The flow stress of high-density polyethylene at high rates of strain. *Polymer Commun.* **26**, 307–308 (1985)
39. Arruda, E.M., Boyce, M.C., Jayachandran, R.: Effects of strain rate, temperature and thermomechanical coupling on the finite strain deformation of glassy polymers. *Mech. Mater.* **19**(2–3), 193–212 (1995)
40. Srivastava, V., Chester, S.A., Ames, N.M., Anand, L.: A thermo-mechanically-coupled large-deformation theory for amorphous polymers in a temperature range which spans their glass transition. *Int. J. Plast.* **26**(8), 1138–1182 (2010)
41. Frank, G.J., Brockman, R.A.: A viscoelastic–viscoplastic constitutive model for glassy polymers. *Int. J. Solids Struct.* **38**, 5149–5164 (2001)
42. Kaliske, M., Rothert, H.: Formulation and implementation of three-dimensional viscoelasticity at small and finite strains. *Comput. Mech.* **19**, 228–239 (1997)
43. Simulia, D.S.: writing user subroutine with Abaqus. *Abaqus* **53**(9), 1689–1699 (2013)
44. Su, T., Zhou, H., Zhao, J., Liu, Z., Dias, D.: A fractional derivative-based numerical approach to rate-dependent stress–strain relationship for viscoelastic materials. *Acta Mech.* **232**, 2347–2359 (2021)
45. Xia, Z., Shen, X., Ellyin, F.: An assessment of nonlinearly viscoelastic constitutive models for cyclic loading: the effect of a general loading/unloading rule. *Mech. Time-Depend. Mater.* **9**, 79–98 (2005)
46. Xia, Z., Hu, Y., Ellyin, F.: Deformation behavior of an epoxy resin subject to multiaxial loadings. Part II: Const. Model. *Predict. Polymer Eng. Sci.* **43**, 734–748 (2003)
47. Lai, J., Bakker, A.: 3-D Schapery representation for nonlinear viscoelasticity and finite element implementation. *Comput. Mech.* **18**, 182–191 (1996)
48. Popelar, C.F., Liechti, K.M.: A distortion-modified free volume theory for nonlinear viscoelastic behavior. *Mech. Time-Depend. Mater.* **7**, 89–141 (2003)
49. Ellyin, F.: *Fatigue Damage, Crack Growth, and Life Prediction*, pp. 179–204. Chapman & Hall, London (1997)

**Publisher’s Note** Springer Nature remains neutral with regard to jurisdictional claims in published maps and institutional affiliations.

Springer Nature or its licensor (e.g. a society or other partner) holds exclusive rights to this article under a publishing agreement with the author(s) or other rightsholder(s); author self-archiving of the accepted manuscript version of this article is solely governed by the terms of such publishing agreement and applicable law.